Diffusion of O vacancies near Si:HfO_2 interfaces: An *ab initio* investigation

C. Tang,[1] B. Tuttle,[2] and R. Ramprasad[1]
[1]*Department of Chemical, Materials and Biomolecular Engineering, Institute of Materials Science, University of Connecticut, 97 N. Eagleville Road, Storrs, Connecticut 06269, USA*
[2]*Department of Physics, Penn State Erie-The Behrend College, Erie, Pennsylvania 16563, USA*
(Received 15 March 2007; published 13 August 2007)

The tendency of oxygen vacancies to diffuse and segregate to the Si:HfO_2 interface is evaluated by performing first principles vacancy formation and migration energy calculations at various distances from the interface. These computations indicate that strong thermodynamic and kinetic driving forces exist for the segregation of oxygen vacancies to the interface, providing for a mechanism for the subsequent formation of interfacial phases.

DOI: 10.1103/PhysRevB.76.073306 PACS number(s): 68.35.Fx, 68.35.Ct, 68.35.Dv

Driven by a need for device miniaturization in the microelectronic industry, Hf-based high-permittivity materials (e.g., HfO_2) have gained interest as potential substitutes for conventional SiO_2 gate dielectrics.[1] Nevertheless, the quality of the interface between HfO_2 (or the closely related ZrO_2) and Si has important implications for device performance. While HfO_2 and ZrO_2 are expected to be thermodynamically stable on Si,[1,2] undesired interfacial phases such as silicides, silica, and silicates are known to form,[1–3] strongly depending on the ambient oxygen pressure and the stoichiometry of the deposited HfO_2 (or ZrO_2).[3–9] It has been postulated that segregation to the interface of point defects such as O vacancies and interstitials provides a mechanism for such interfacial phase formation.[9–11]

Recent first principles investigations have increased our understanding of these interfaces at the atomic level.[12–15] General bonding rules to describe the equilibrium atomic level interface structure have been developed[12] and applied to several epitaxial Si:HfO_2 and Si:ZrO_2 interfaces.[12,13] *Ab initio* molecular dynamics simulations that directly address the layer-by-layer nonepitaxial growth of HfO_x on Si (Ref. 15) indicate the tendency for the diffusion of O toward the interface, resulting in the formation of interfacial silica. The resulting Hf dangling bonds appear to be saturated either by Hf diffusion or the formation of Hf-Si bonds.

The present work offers a different perspective to evaluate the tendency for the formation of interfacial phases. A variety of coherent, epitaxial Si:HfO_2 heterostructures is considered, and the propensity for site-to-site O vacancy diffusion is studied through the computation of the formation and migration energies as a function of proximity to the Si:HfO_2 interface. In contrast to the *ab initio* molecular dynamics work,[15] only one process, namely, O vacancy diffusion, is treated here. Nevertheless, this strategy allows us to study this crucial process in a controlled and systematic manner. Our results show quantitatively that the segregation of O vacancies to the interface is favored both thermodynamically and kinetically, indicating a preference for the formation of a Hf silicide layer at the interface in the presence of O vacancies. Although other point defects, including O interstitials, need to be considered as well for a comprehensive understanding of interfacial phase formation, the present work constitutes an initial step toward that goal.

Density functional theory calculations were performed using the VASP code[16] with the Vanderbilt ultrasoft pseudopotentials,[17] the generalized gradient approximation (GGA) utilizing the PW91 functional,[18] and a cutoff energy of 350 eV for the plane wave expansion of the wave functions. A Monkhorst-Pack k-point mesh of $6\times6\times1$ produced well converged results in the case of the smallest interface models that contained one Si atom per layer, and the k-point mesh was proportionately decreased for larger supercells.

In this work, we mainly focus on O-terminated interfaces because they are more stable and desirable than Hf-terminated ones.[12] Specifically, three interface models studied earlier,[12,13] and another one based on monoclinic HfO_2 were considered here. In all cases, a (001) HfO_2 slab was coherently matched on top of a (001) Si slab at its equilibrium GGA lattice constant of 5.46 Å. In contrast to prior work,[12] a vacuum region of about 10 Å separated a heterostructure from its periodic images to adequately allow for surface and interface reconstructions. The top (Hf) and bottom (Si) free surfaces were passivated with half monolayer of O atoms, thereby saturating all surface dangling bonds.[12] Our Si:HfO_2 heterostructures can, thus, be represented as $O(HfO_2)_mSi_nO$, where the O in either end are the passivating layers, and m and n represent the number of Hf and Si layers, respectively.

The four Si:HfO_2 heterostructures considered here are labeled a–d. Heterostructure a (designated as O_4 in Ref. 12 and a in Ref. 13) was created by placing a cubic HfO_2 slab on Si such that the [100] directions of both Si and HfO_2 coincide with each other. Consistent with the bond counting arguments of Peacock *et al.*,[12] geometry optimization shows that half the interface O atoms move downward, creating Si-O-Si bonds, and the other half move upward creating Hf-O-Hf bonds, as shown in Fig. 1(a). The resulting structure can, thus, be represented as $O(HfO_2)_{(m-1)}HfOOSi_nO$, highlighting the splitting up of the interfacial O layer. This "rumpling" of the O layers persists into the HfO_2 part, resulting in a structure equivalent to tetragonal HfO_2. Heterostructure b (labeled as O_3 in Ref. 12 and b in Ref. 13) was constructed from heterostructure a by translating the HfO_2 slab along with the Hf-O-Hf units at the interface along the [010] direction by $a/2$, where a is the primitive lattice constant of Si (3.86 Å). Geometry optimization shows that the lowest layer of interface O atoms are bound to two Si and one Hf atoms, again

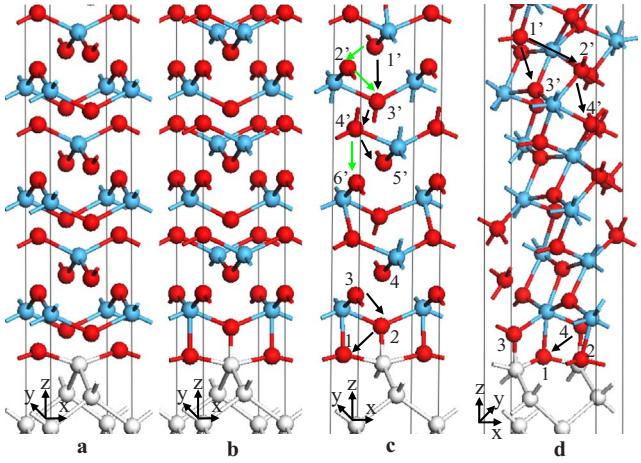

FIG. 1. (Color online) Models of heterostructures a, b, c, and d. Si, Hf, and O atoms are represented as white, blue (gray), and red (dark gray) spheres, respectively. Isolated O vacancies were created at the labeled O sites, and arrows represent the migration pathways for O vacancies.

resulting in tetragonal HfO_2 away from the interface. Heterojunction c (similar to the O_{3T} model of Ref. 12) was obtained from heterostructure a by translating the HfO_2 slab along with the Hf-O-Hf units along [010] by $a/4$. Optimization of this structure resulted in an interface similar to that of b as can be seen in Fig. 1. However, the HfO_2 away from the interface was unlike any of the equilibrium HfO_2 structures, as discussed more below.

Heterojunction d was constructed by placing monoclinic HfO_2 on Si such that the [100] direction of HfO_2 coincided with that of Si. Geometry optimization of this model results in a structure with the lowest symmetry at the interface. Near the interface, the O layers are also split up (like a–c), but away from the interface the monoclinic phase of HfO_2 is preserved [Fig. 1(d)].

Table I lists the total energies (E_{tot}) of all heterostructures studied *relative* to that of heterostructure a, for two different HfO_2 thicknesses. For the thinner HfO_2 case ($m=4$), E_{tot} of b, c, and d are lower than that of a by 1.94, 2.95, and 4.06 eV, respectively. Increasing the HfO_2 thickness to $m=8$ results in a small change in the E_{tot} of b relative to that of a, but those of c and d change significantly. This is not surprising as HfO_2 away from the Si:HfO_2 interface in the cases of a and b has tetragonal symmetry, whereas in the cases of c and d, HfO_2 has a more stable, lower symmetry structure. Thus, the high stability of c and d are in part due to the more stable phases of HfO_2 they contain.

TABLE I. Total energies (E_{tot}) and cleavage energies (E_{clea}) relative to a (in eV) per 3.86×3.86 Å^2 of interface area for heterostructures with two different HfO_2 layer thicknesses. Nine Si layers were used in all cases, and m represents the number of Hf layers.

	E_{tot}		E_{clea}	
Heterostructure	$m=4$	$m=8$	$m=4$	$m=8$
a	0	0	0	0
b	−1.94	−1.86	1.94	1.89
c	−2.95	−4.58	1.92	1.82
d	−4.06	−5.08	0.43	0.25

In order to factor out the role played by the "bulk" HfO_2 part of the heterostructures and to directly address the relative stability of the interface regions, the cleavage energy (E_{clea}) required to separate a heterostructure into two parts is considered.[19] E_{clea} is defined as the energy of the following reaction:

$$O(HfO_2)_{m-1}HfOOSi_nO \rightarrow O(HfO_2)_{m-1}HfO + OSi_nO. \quad (1)$$

The geometry of the "products" of the above reaction for all heterostructures were optimized. Table I also lists E_{clea} for all heterojunctions, again relative to that of heterostructure a. Regardless of HfO_2 thickness, it is clear that b–d have Si:HfO_2 interfaces more stable than that of a. E_{clea} of b and c are nearly identical, indicating the similarity of their interfacial configuration. E_{clea} of d is lower than those of b and c, reflecting the more disordered interface between Si and monoclinic HfO_2. The rest of this Brief Report will focus on heterostructures c and d owing to their higher stability and stable Si:HfO_2 interfaces.

O vacancy formation energies, E_{form}, were calculated for vacancies at various distances from the Si:HfO_2 interfaces in heterostructures c and d. Vacancies at sites close to the interface labeled by unprimed indices in Fig. 1 were treated using the entire heterostructure geometry ($m=4$), with dimensions of 10.92×10.92 Å^2 along the interface plane. Those at sites away from the interface labeled by the primed indices in Fig. 1 were treated using bulk HfO_2 supercells extracted from c and d. Bulk HfO_2 corresponding to c had two- and threefold coordinated O sites, and the monoclinic phase (corresponding to d) had three- and fourfold coordinated O sites.

E_{form} was defined as $E_{form}=E_{vac}+(E_{O_2}/2)-E_{perf}$, where E_{vac}, E_{O_2}, and E_{perf} are the energies of the system with an O vacancy, an isolated O_2 molecule, and a vacancy-free system, respectively. The computed E_{form} values are listed in Table II. For both c and d, E_{form} is highest in the bulk and almost monotonically decreases by over 1 eV as the interface is approached. This reflects the thermodynamic driving force for the tendency of O vacancies to migrate to the interface from the bulk. The trend of decreasing defect formation energy with proximity to the interface is consistent with previous results for Si:HfO_2 (Refs. 14 and 15) and other oxide[20] interfaces.

Despite the thermodynamic driving force, whether O vacancies will actually segregate to the interface will be determined by the barriers to site-to-site migration of O vacancies. In order to address such kinetic factors in detail, O vacancy migration calculations were performed using the nudged elastic band method[21] for the same supercells used for E_{form} calculations. Energy barriers for migration, E_{migr}, along the pathways shown by arrows in Fig. 1 were determined for c and d, and are listed in Table II. E_{migr} for the bulk HfO_2 phase, corresponding to c, is in the 1.67–2.41 eV range, depending on the migration path. For example, a va-

TABLE II. Vacancy formation (E_{form}) and migration (E_{migr}) energies (eV) in bulk HfO_2 and near interface. Refer to Fig. 1 for the labels of vacancy sites and migration paths.

	Bulk HfO_2				Near interface			
	Vacancy site	E_{form}	Migration path	E_{migr}	Vacancy site	E_{form}	Migration path	E_{migr}
c	Twofold (1′ and 2′)	5.86	1′ to 2′	2.40	4	5.39		
			1′ to 3′	2.02	3	5.48	3 to 2	1.38
			2′ to 3′	1.69	2	4.45	2 to 1	0.52
	Threefold (3′ and 4′)	5.48	3′ to 4′	1.67	1	4.19		
			4′ to 5′	2.04				
			4′ to 6′	2.41				
d			1′ to 2′	2.41	4	6.14	4 to 1	0.88
	Threefold (1′ and 3′)	6.48	1′ to 3′	1.62	3	5.95		
	Fourfold (2′ and 4′)	6.24	2′ to 4′	1.95	2	5.33		
					1	5.16		

cancy at the 1′ (twofold) site of c can directly migrate to the 3′ (threefold) site with a barrier of 2.02 eV, or through a two-step process via an intermediate twofold site (2′) with barriers of 2.40 and 1.69 eV. Near the interface, the barriers from site 3 to site 2 and then to site 1 were computed to be 1.38 and 0.52 eV, respectively, for heterostructure c. The rather large drop in the barrier energies as the interface is approached is, thus, evident. The E_{migr} values for c, along with the E_{form} values, were used to create an O vacancy migration energy profile shown in Fig. 2 (top). All energies in this figure represented as square symbols correspond to those of the "images" of the nudged elastic band computations (i.e., initial, final, and intermediate geometric configurations during migration). Energies are defined relative to $[(E_{O_2}/2)-E_{perf}]$, so that the minima of this profile correspond to vacancy formation energies. Figure 2 pictorially

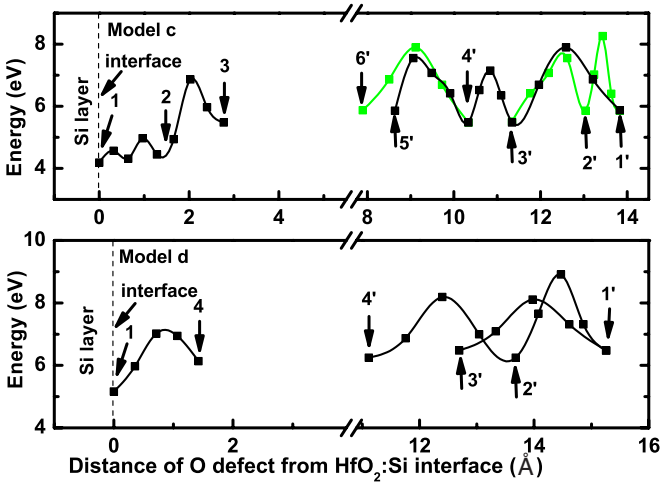

FIG. 2. (Color online) O vacancy migration profiles for model c and model d. Primed and unprimed indices correspond to those in Figs. 1(c) and 1(d). The green (gray) and black curves correspond to the green (gray) and black arrow paths in Fig. 1(c). The vertical dashed line indicates the location of the interface, with Si to the left.

captures *both* the thermodynamic and kinetic driving forces for the segregation of O vacancies to the interface.

As shown in Table II, the migration energies in the bulk HfO_2 phase, corresponding to heterostructure d, are in the 1.62–2.41 eV range, almost identical to that for c. Also, E_{migr} for migration between two threefold sites ($1' \rightarrow 3'$) in this case is 1.62 eV, which is almost identical to that between two threefold sites ($3' \rightarrow 4'$) of c. It, thus, appears that regardless of the actual nature of the phase, the local chemistry and coordination environment determine defect properties. Close to the interface, the barrier for migration from site 4 to site 1 was computed to be 0.88 eV. Figure 2 (bottom) shows the migration energy profile for d. The qualitative features of Fig. 2 (top) are reproduced in this profile, although the actual values of the barriers are different.

Recent *ab initio* molecular dynamics calculations that simulate the layer-by-layer growth of HfO_2 on Si indicate that the interfacial O atoms from O-deficient HfO_2 tend to diffuse to the Si side.[15] However, it has been pointed out that the relocation of lattice O from HfO_2 to Si, creating Si-O-Si bonds, is endothermic,[22] especially when HfO_2 is O deficient.[3] In order to explore these possibilities, we considered c in the absence of any O vacancies initially and relocated a lattice O atom from site 2 to the equilibrium location in the middle of the Si-Si bond below. We found that this process is endothermic by 0.87 eV, with a barrier of 1.21 eV. Molecular dynamics simulations at a temperature of 1000 K and for a time step of 3 fs were also performed for c, with an O vacancy initially at site 2 [Fig. 1(c)]. At about the 500th time step, the O atom from site 1 filled the vacancy, and for the subsequent 1500 time steps, the vacancy continued to be at site 1. Thus, our results imply that Si oxidation (i.e., formation of Si-O-Si bonds) by stoichiometric or O-deficient HfO_2 is improbable, at least in the case of coherent epitaxial $Si:HfO_2$ heterostructures.

In summary, we have performed detailed first principles computations on several $Si:HfO_2$ models both to assess their relative stability and to understand the tendency for the atomic level diffusion of O vacancies in such heterostructures. Regardless of the actual interface model employed, a

general conclusion that emerges is that strong thermodynamic *and* kinetic driving forces exist for the segregation of O vacancies to the interface. Thus, although stoichiometric O-terminated $Si:HfO_2$ interfaces are expected to be stable, point defects such as O vacancies may render these interfaces unstable to the formation of Hf silicides due to the accumulation of O vacancies at the interface, consistent with prior experimental work.[4,6,8] It is also expected that the insights that have emerged from this work are quite general. Although coherent crystalline heterojunctions were considered, the defect properties studied here are determined largely by the local coordination environment rather than long range order.

The authors would like to acknowledge financial support of this work by the ACS Petroleum Research Fund.

[1] R. M. Wallace and G. D. Wilk, Crit. Rev. Solid State Mater. Sci. **28**, 231 (2003).
[2] J. Robertson, Rep. Prog. Phys. **69**, 327 (2006).
[3] N. Miyata, Appl. Phys. Lett. **89**, 102903 (2006).
[4] D. Y. Cho, K. S. Park, B. H. Choi, S. J. Oh, Y. J. Chang, D. H. Kim, T. W. Noh, R. Jung, J. C. Lee, and S. D. Bu, Appl. Phys. Lett. **86**, 041913 (2005).
[5] D. Y. Cho, S. J. Oh, Y. J. Chang, T. W. Noh, R. Jung, and J. C. Lee, Appl. Phys. Lett. **88**, 193502 (2006).
[6] X. Y. Qiu, H. W. Liu, F. Fang, M. J. Ha, and J. M. Liu, Appl. Phys. Lett. **88**, 072906 (2006).
[7] H. S. Baik, M. Kim, G.-S. Park, S. A. Song, M. Varela, A. Franceschetti, S. T. Pantelides, and S. J. Pennycook, Appl. Phys. Lett. **85**, 672 (2004).
[8] Y. Y. Lebedinskii, A. Zenkevich, E. P. Gusev, and M. Gribelyuk, Appl. Phys. Lett. **86**, 191904 (2005).
[9] C. M. Perkins, B. B. Triplett, P. C. McIntyre, K. C. Saraswat, and E. Shero, Appl. Phys. Lett. **81**, 1417 (2002).
[10] S. Ferrari and G. Scarel, J. Appl. Phys. **96**, 144 (2004).
[11] J. Y. Dai, P. F. Lee, K. H. Wong, H. L. W. Chan, and C. L. Choy, J. Appl. Phys. **94**, 912 (2003).
[12] P. W. Peacock, K. Xiong, K. Tse, and J. Robertson, Phys. Rev. B **73**, 075328 (2006).
[13] Y. F. Dong, Y. P. Feng, S. J. Wang, and A. C. H. Huan, Phys. Rev. B **72**, 045327 (2005).
[14] J. L. Gavartin, L. Fonseca, G. Bersuker, and A. L. Shluger, Microelectron. Eng. **80**, 412 (2005).
[15] M. H. Hakala, A. S. Foster, J. L. Gavartin, P. Havu, M. J. Puska, and R. M. Nieminen, J. Appl. Phys. **100**, 043708 (2006).
[16] G. Kresse and J. Furthmuller, Phys. Rev. B **54**, 11169 (1996).
[17] D. Vanderbilt, Phys. Rev. B **41**, R7892 (1990).
[18] J. P. Perdew, J. A. Chevary, S. H. Vosko, K. A. Jackson, M. R. Pederson, D. J. Singh, and C. Fiolhais, Phys. Rev. B **46**, 6671 (1992).
[19] I. G. Batirev, A. Alavi, M. W. Finnis, and T. Deutsch, Phys. Rev. Lett. **82**, 1510 (1999).
[20] D. C. Sayle, T. X. T. Sayle, S. C. Parker, C. R. A. Catlow, and J. H. Harding, Phys. Rev. B **50**, 14498 (1994).
[21] G. Henkelman and H. Jonsson, J. Chem. Phys. **113**, 9978 (2000).
[22] K. Shiraishi, K. Yamada, K. Torii, Y. Akasaka, K. Nakajima, M. Konno, T. Chikyow, H. Kitajima, T. Arikado, and Y. Nara, Thin Solid Films **508**, 305 (2006).